Journal of Hydrology 528 (2015) 435–448

Contents lists available at ScienceDirect

Journal of Hydrology

journal homepage: www.elsevier.com/locate/jhydrol

Interaction between groundwater and trees in an arid site: Potential impacts of climate variation and groundwater abstraction on trees

Lihe Yin [a,b,*], Yangxiao Zhou [b], Jinting Huang [a], Jochen Wenninger [b,c], Eryong Zhang [d], Guangcai Hou [a], Jiaqiu Dong [a]

[a] Xi'an Center of Geological Survey, China Geological Survey, No. 438, Youyidong Road, Xi'an 710054, China
[b] UNESCO-IHE Institute for Water Education, P.O. Box 3015, 2601 DA Delft, The Netherlands
[c] Delft University of Technology, Faculty of Civil Engineering and Geosciences, Water Resources Section, Stevinweg 1, 2628 CN Delft, The Netherlands
[d] China Geological Survey, No. 45, Fuwai Street, Beijing 100037, China

ARTICLE INFO

Article history:
Received 31 March 2015
Received in revised form 10 June 2015
Accepted 28 June 2015
Available online 2 July 2015
This manuscript was handled by Peter K. Kitanidis, Editor-in-Chief, with the assistance of J. Simunek, Associate Editor

Keywords:
Groundwater use
Tree water uptake
Arid regions
HYDRUS-1D
Stable isotopes
Groundwater abstraction

SUMMARY

The understanding of the interaction between groundwater and trees is vital for sustainable groundwater use and maintenance of a healthy ecosystem in arid regions. The short- and long-term groundwater contribution to tree water use was investigated using the HYDRUS-1D model and stable isotopes. For the short-term simulation, the ratio between the actual transpiration (T_a) and potential transpiration (T_p) approached almost ~1.0 due to the constant groundwater uptake. The results from the short-term simulation indicated that the groundwater contribution to tree water use ranged between 53% and 56% in the dry season (May–June) and 16–19% in the wet period (August–September). Isotopic analysis indicated that groundwater contributed to 45% of plant water use in the dry season, decreasing to 4–12% during the wet period. Because of canopy interception and transpiration, groundwater recharge only occurred after heavy rainfall and accounted for 3–8% of the total heavy rainfall. For the long-term simulation, T_a/T_p ranged between 0.91 and 1.00 except in 2007 (0.78), when the water table declined because of groundwater abstraction. In the scenario simulation for deep water table conditions caused by anthropogenic activities, T_a/T_p ranged between 0.09 and 0.40 (mean = 0.22) that is significantly lower than the values in the natural conditions. In conclusion, vegetation restoration in arid zones should be cautious as over-planting of trees will decrease the groundwater recharge and potentially cause a rapid drop in water table levels, which in turn may result in the death of planted trees. Trees adapt to arid regions by adopting root patterns that allow soil water uptake by shallow roots and groundwater use by deep roots, thus climatic variation itself may not bring severe negative impact on trees. However, anthropogenic activities, such as groundwater abstraction, will result in significant water table decline that will reduce actual transpiration of trees significantly according to the results from the scenario simulation.

1. Introduction

Arid regions cover about one third of the Earth's land surface and are inhabited by almost one billion people (Yin et al., 2013). In arid environments, trees play a significant role in maintaining those environments suitable for agriculture and humans (Malagnoux et al., 2007) by providing natural protection against desertification (Tucker et al., 1991) and reducing poverty and food insecurity (Schreckenberg et al., 2006). Therefore, the majority of the newly afforested 100 million hectares during the period of 2000–2010 is located in arid zones and particularly in arid zones of China (FAO, 2010). As an example, several large-scale ecological restoration projects have been carried out in Chinese arid regions, including the Three North Shelter Belts Forest, the Grain for Green, and the Natural Forest Conservation projects (Cao, 2011).

Water, including surface water, groundwater, and soil water, is vital for tree growth (Zhu et al., 2009 and Richard et al., 2013), with groundwater being an important source in arid regions as it is relatively constant and stable. Many trees in arid regions are reported to be groundwater-dependent (Bulter et al., 2007 and Gribovszki et al., 2010) and they can obtain large amounts of groundwater for transpiration through deep roots, especially during dry seasons (David et al., 2007 and Lubczynski, 2009).

The contribution of groundwater to plant water use has been studied for a long time, with a pioneering study from White

* Corresponding author at: Xi'an Center of Geological Survey, China Geological Survey, No. 438, Youyidong Road, Xi'an 710054, China. Tel.: +86 29 87821986; fax: +86 29 87821978.
E-mail address: ylihe@cgs.cn (L. Yin).

http://dx.doi.org/10.1016/j.jhydrol.2015.06.063
0022-1694/

(1932). Nevertheless, most studies focused on the estimation of groundwater use by crops (e.g., winter wheat, corn, and cotton) and vegetables (e.g., potato) to reduce the water use and enhance the irrigation efficiency in water-limited environments (Xie et al., 2011). For example, in many agricultural areas in China (Yang et al., 2007 and Luo and Sophocleous, 2010) and Uzbekistan (Forkutsa et al., 2009), the water table is located less than 1.0 m below the surface due to the infiltration of irrigated surface water. In these regions, groundwater is a major source for plant transpiration and over 60% of water use originates from shallow groundwater (Luo and Sophocleous, 2010 and Karimov et al., 2014). However, the understanding of the groundwater contribution to tree water use in natural environments is limited. Examples are the study of Zhu et al. (2009), who simulated the *Populus euphratica* root uptake of groundwater in arid woodlands of the Ejina Basin, China, and of Costelloe et al. (2008), who studied the groundwater contribution to *Eucalyptus coolabah* water uptake in Australia. Recently, Barbeta et al. (2015) studied the shift of groundwater contribution to *Quercus ilex*, *Arbutus unedo* and *Phillyrea latifolia* in the Lberian Peninsula, Spain. In the regional scale, water table decline resulted in the reduction of groundwater contribution to trees and the dieback of trees occurred accordingly (Cunningham et al., 2011 and Kath et al., 2014). As trees have deeper roots and no irrigation in comparison to crops, they are more dependent on groundwater and more sensitive to the water table drops, particularly during dry seasons (Zhu et al., 2009 and Pinto et al., 2014).

Trees reduce groundwater recharge by canopy interception and by extracting soil water (Maitre et al., 1999). Canopy interception corresponds to the rainfall retained by the plant's surface that evaporates directly back into the atmosphere (Sutanudjaja et al., 2011). Controlled by meteorological and canopy architecture factors, canopy interception losses generally vary between 10% and 40% of annual precipitation (Zinke, 1967; Waring and Schlesinger, 1985; Farrington and Bartle, 1991 and Xiao et al., 2000). However, canopy interception is often ignored in groundwater–vegetation interaction studies (Sutanto et al., 2012). Groundwater recharge is also reduced due to the use of soil water by trees (Asbjornsen et al., 2011), an unsaturated flow modeling study shows that vegetation significantly reduce recharge by factors of 2–30 relative to recharge for nonvegetated simulations (Keese et al., 2005). Trees reduce groundwater resources and are groundwater-dependent in arid regions, therefore, the understanding of the interaction between them is critical. These complex groundwater–tree interactions complicate the development of water allocation plans that take into account the various anthropogenic and ecosystem water uses (Kløve et al., 2013) and the appropriate selection of tree species that reduce groundwater consumption in the afforestation of water-limited environments (Yin et al., 2014). More investigation is thus needed to maintain healthy ecosystems and achieve a sustainable use of groundwater in arid regions.

The interaction between groundwater and plants is widely studied using lysimeters (Kelleners et al., 2005 and Wenninger et al., 2010), which can simultaneously measure the components of the water balance. However, they involve high costs and limited observation periods. Modeling becomes a valuable tool to quantify the groundwater–plant interactions as many models can simulate the root water uptake (Scanlon et al., 2002 and Soylu et al., 2011). Modeling methods allow the study of the long-term interactions and the response of plant water use to various climatic, water table depth, and anthropogenic conditions (Luo and Sophocleous, 2010). Long-term simulations at decades scale are vital to study the plant adaptation to local environments. The advantage of numerical methods is the high temporal resolution (hours or days) of the groundwater contribution to plant water use (Scanlon et al., 2002 and Sutanto et al., 2012), with a daily resolution being commonly adopted (Luo and Sophocleous, 2010 and Xie et al., 2011). Furthermore, it is the only tool that can be used to predict the potential impacts of water table changes caused by climatic variation or human activities on plant water use (Luo and Sophocleous, 2010). However, the soil water balance components calculated from model results contain uncertainty, as models need many parameters to describe boundary conditions, drought stress parameters and soil properties, which often have to be assumed (Lu et al., 2011). For example, the lower boundary for long-term simulations is usually given by the assumed water table due to data limitations, even though previous studies have suggested that plant water use is very sensitive to its fluctuations (Leyer, 2005; Zhu et al., 2009; Luo and Sophocleous, 2010 and Ibrahimi et al., 2013). In currently available numerical methods, the groundwater contribution is estimated indirectly and the positive bottom flux is assumed to be the groundwater contribution to plant transpiration, but this assumption may be incorrect under a very shallow water table or very fine soil, because part of the bottom flux may evaporate (Lubczynski, 2009).

Stable water isotopes can be used to directly estimate the groundwater contribution and are another important technique to study the interaction between groundwater and plants. As no fractionation occurs during the water uptake by roots (Zimmermann et al., 1967), the stem water can be considered as a mixture of the potential water sources (i.e., soil water at different depths and groundwater). The proportional contribution of the different water sources can then be estimated using two- or three-layer mixing models (McCole and Stern, 2007 and Wang et al., 2010). For more than three water sources, a multi-source mass balance method must be used (Phillips and Gregg, 2003). The limitations of this method include the low temporal resolution (months–seasons) (Zencich et al., 2002 and Wang et al., 2013), the uncertainty with more than two potential sources (Phillips and Gregg, 2001), and the assumption of isotopically distinct water sources (Obakeng, 2007 and Lubczynski, 2009). Nonetheless, previous studies showed that this method is powerful during dry periods when the soil water is enriched and isotopically distinct from groundwater.

The objective of the study is to investigate the interaction between groundwater and willow trees (*Salix matsudana*) in an arid experimental site of NW China and to address knowledge gaps on the drivers and impacts of tree–groundwater interaction in arid regions. The study focuses on groundwater contribution to tree water use, groundwater recharge reduction due to tree canopy interception and the use of soil water, and the impact of water table changes caused by climatic variation and anthropogenic activities on tree water use. Isotopic and numerical modelling methods were used to investigate groundwater–tree interactions. The numerical modelling method was used to calculate the contribution of groundwater to plant water uptake at a high temporal resolution and to assess the anthropogenic influence on plants, while the isotopic method was applied to dry periods to validate the numerical estimations.

2. Materials and methods

2.1. Study site

The study area is located in an eco-hydrological experimental site near Yulin, Shaanxi province, NW China (latitude: 38°23′N, longitude: 109°12′E, altitude: 1250.5 m) and the site covers an area about 80 m × 35 m (Fig. 1). Historical records from 1985 to 2010 for the region indicate that the annual precipitation has varied from 249 mm to 579 mm, with an average of 385 mm and a standard deviation of 85 mm. About 70% of the precipitation occurs in

Fig. 1. The experimental site map showing the location of instruments.

July–September. The farmland surrounding the site is irrigated by groundwater and surface water from a river through canal systems. When the river flow is low due to continuous dry weather, groundwater is used heavily for irrigation. The dominated tree in the site is willow (*S. matsudana*) with a few populous trees. The total number of willow trees are 107 and they were planted in rows in the 1970s (Yin et al., 2014), and the distance between rows is about 5 m and the distance between trees in a row is 4 and 6 m. The mean height of the willow trees is 4.6 ± 0.8 m and the mean diameter at breast height is 0.23 ± 0.06 m. In 2012, the main understory was native herbs and grasses. The soils are composed of eolian and lacustrine sands with a thickness of ~50 m. Below the sand layer, Cretaceous and Jurassic sandstones can be found, with the latter containing abundant coal resources. Future coal mining in the study site may result in a significant drop in water table (Bian et al., 2009). The depth to water table was rather shallow, ranging from 1.1 to 1.7 m during the study period and the hydraulic gradient of the region was about 0.4%.

2.2. Experimental set-up

A suite of variables has been measured at the site and Fig. 1 shows the instrument locations. The meteorological variables measured at the site included precipitation, wind speed, air temperature, relative humidity, and net radiation. The precipitation rate (in mm/h) was recorded using a 52203 RM Young rain gauge (R.M. Young Co., Michigan, USA) and the wind speed (in m/s) was measured with a 05130-5 RM Young wind monitor (R.M. Young Co., Michigan, USA) located 5.3 m above the ground. The air temperature (in °C) and relative humidity (in %) were measured with a thermo-hygrometer (HMP45C,Vaisala Co., Helsinki, Finland) at 4.3 m height. The net radiation (in W/m^2) was measured using a NR-LITE sensor (Kipp & Zonen, Delft, The Netherlands). One soil water profile was monitored (Fig. 1) using a Time Domain Reflectometry System (MiniTrase, Soilmoisture Equipment Corp., Santa Barbara, CA, USA), with sensors positioned 20, 40, 60, 80, 100, 120, 140, and 160 cm below the surface. The water table depth was measured in one well (Fig. 1) using a pressure transducer and data logger (Model DCX-22, KELLER AG für Druckmesstechnik, Winterthur, Switzerland). All parameters were measured hourly between May 2 and September 26, 2012. The long-term meteorological data (1985–2010) were obtained from the nearest Yulin meteorological station. The long-term groundwater level in an observation well was measured manually every 5 days from 1992 to 2010.

Water samples were collected for stable isotopes analysis (deuterium and oxygen 18). The precipitation samples were collected during rainfall events. Stem water, soil water, and groundwater were sampled every 10 days. Stem water was extracted by the vacuum distillation method (Zhang et al., 2011) from a willow tree nearest to the soil water profile. Soil water was collected from the soil water profile by eight Rhizon soil water samplers (Eijkelkamp Agrisearch Equipment, Giesbeek, The Netherlands) at the depth of 20, 40, 60, 80, 100, 120, and 140. Groundwater was collected by the deepest Rhizon sampler (i.e. the sampler at 160 cm depth) where soil was fully saturated during the entire experimental period. The water samples were analyzed by a LGR liquid water isotope analyzer (LWIA-24d, Los Gatos Research, CA, USA) and the results were reported as per mil deviations from the Vienna Standard Mean Ocean Water (VSMOW). The IsoSource multiple-source isotopic mass balance model was use to determine the potential source of tree water use, and the theory and calculation procedure are after Phillips and Gregg (2003) and Phillips et al. (2005).

2.3. Model construction

The HYDRUS-1D (Šimůnek et al., 2013) was selected to simulate the interaction between groundwater and plants, as previous studies showed a good agreement between water balance observations and simulations based on this model (Scanlon et al., 2002 and Zhu et al., 2009). Three model cases were performed. The first model was a short-term simulation (May 2–September 26, 2012) to calibrate and validate the model parameters using the measured data in the experimental site. The groundwater contribution to tree water use was analyzed by compute the soil water balance based on the model results. The second model was a long-term simulation (1992–2010) using the parameters calibrated from the first model and the measured groundwater levels in an observation well and meteorological variables from the nearest station. The representativeness of the climate for the selected period (1992–2010) was compared with the measured annual precipitation for 1953–2010, based on the method developed by Blom (1958). The second model aims to assess the potential impact of long-term climatic variation on tree water use. The third model was a scenario simulation to assess the impact of a deep water table condition caused by anthropogenic activities, such as coal mining or groundwater abstraction, on plant water use.

2.3.1. Governing water flow equations

The HYDRUS-1D simulates the water flow in variably saturated porous media using the Richards equation:

$$\frac{\partial\theta}{\partial t}=\frac{\partial}{\partial z}\left[k(\theta)\frac{\partial h}{\partial z}+k(\theta)\right]-S(z,t) \tag{1}$$

where θ is the volumetric water content (cm^3/cm^3), t is time (days), z is the vertical coordinate (positive upward) (cm), $k(\theta)$ is the unsaturated hydraulic conductivity (cm/d), h is the matric potential head (cm), and S is the extraction rate by plant roots ($cm^3/cm^3/d$). The relationships between θ, h, and k are required to solve the equation (Brooks and Corey, 1966 and van Genuchten, 1980) and are described using van Genuchten's (1980) functions:

$$\theta(h)=\begin{cases}\theta_r+\frac{\theta_s-\theta_r}{(1+|\alpha h|^n)^m}, & h<0\\ \theta_s, & h\geqslant 0\end{cases} \tag{2}$$

$$k(h)=k_s S_e^l\left[1-\left(1-S_e^{\frac{1}{m}}\right)^m\right]^2 \tag{3}$$

where θ_r and θ_s are the residual and saturated water contents (cm^3/cm^3), α (cm), n, and m (=1 − 1/n) are shape parameters, l is a pore connectivity parameter, k_s is the saturated hydraulic conductivity and S_e is the effective saturation, defined as:

$$S_e=\frac{\theta-\theta_r}{\theta_s-\theta_r} \tag{4}$$

2.3.2. Spatial and temporal discretization

The model flow domain extended to 3.5 m below the land surface, deeper than the root zone and at the lowest water table observed in the area. The soil column of 3.5 m is descretised into 350 model cells with a constant cell size of 0.01 m. The short-term simulation was from May 2 to September 26, 2012 during which the meteorological variables, soil water content, and water table depth were measured hourly. For the long-term and scenario simulations (1992–2010), the simulation only included the plant-growing season (April–October) as the willow trees lost their leaves and the transpiration rate is close to zero during the rest of the year indicated by the previous study (Yin et al., 2014). A daily time-step was used for all simulations.

2.3.3. Initial and boundary conditions

The solution of Eq. (1) requires initial and boundary conditions. For the short-term simulation, the initial condition was defined as the soil water content measured on day 1 of the experiment. For the long-term simulation, it was assumed to be in equilibrium with the water table measured on day 1 and the assumption is valid considering the relatively shallow depth of water table. For the scenario simulation, the model was run until the soil water profile was stable, and the resultant value was used.

The lower boundary was defined as a specified head boundary for the short- and long-term simulations. The measured groundwater levels in the experimental site and an observation well were given as specified heads for the short- and long-term simulations, respectively. A free drainage lower boundary was defined for the scenario simulation to represent the deep water table condition. The upper boundary was specified as an atmospheric boundary for all simulations. A default value (i.e., 100,000 cm) was used as the dry value that controls the change of the upper boundary from a prescribed head to a prescribed flux and vice versa (Lu et al., 2011). Our results were not sensitive to this threshold value. Runoff occurred when precipitation exceeded the infiltration capacity of the soil. The flux through the upper boundary included the effective precipitation and evaporation. The effective precipitation (P_e) was calculated as the difference between the gross precipitation (P_g) and the canopy interception (I). The P_g was measured by an in situ rain gauge and the I was estimated by a daily interception method (van Dam et al., 1997):

$$I=a\mathrm{LAI}\left(1-\frac{1}{1+\frac{bP_g}{a\mathrm{LAI}}}\right) \tag{5}$$

where a is an empirical constant (cm/d), LAI is the leaf area index (m^2/m^2), and b is the surface cover fraction (SCF) derived from MODIS imagery (MOD13A1) using the dimidiate pixel model (Zribi et al., 2003). According to previous canopy interception studies in similar environments (Cheng et al., 2009 and Wang et al., 2012), a was set as 0.5 cm/d.

The Penman–Monteith equation was used to calculate the potential evapotranspiration (ET_p) (Allen et al., 1998). The values of meteorological variable (such as air temperature, relative humid, net radiation and wind speed) in the Penman–Monteith equation are obtained from the measured data.

The site-specific vegetation parameters (tree height and LAI) for the aerodynamic and canopy resistance were derived from field surveys or remote sensing imagery. The tree height was measured using a tape and the LAI was inferred from the MODIS LAI products (MOD15A2).

The Beer's law method was used to partition ET_p into the potential transpiration (T_p) and potential evaporation (E_p) as follows (Sutanto et al., 2012 and Šimůnek et al., 2013):

$$T_p=ET_p\times \mathrm{SCF} \tag{6}$$

$$E_p=ET_p\times(1-\mathrm{SCF}) \tag{7}$$

2.3.4. Plant water uptake

The plant water uptake from Eq. (1) was simulated by:

$$S=\alpha(h)T_p c(z) \tag{8}$$

where $\alpha(h)$ is the water stress response function and $c(z)$ is the normalized vertical root distribution (cm^{-1}). The S-shaped function (van Genuchten, 1987) was used to describe the water stress response as it has been widely used to represent the water stress response function of trees (Zhu et al., 2009 and Richard et al., 2013):

$$\alpha(h)=\frac{1}{1+\left(\frac{h}{h_{50}}\right)^p} \tag{9}$$

where h_{50} is the pressure head (cm) at which transpiration is reduced by 50% and p is the exponent parameter. h_{50} was calibrated and p was set to 3 according to Šimůnek et al. (2013).

The root distribution of the willow tree from which stem water was collected was determined with a root auger (Eijkelkamp Agrisearch Equipment, Giesbeek, The Netherlands). Soil core samples were taken at two stem-centered cross-sections, each with eight sampling points. The root samples at each point were excavated every 15 cm depth at a maximum sampling depth of 150 cm. The samples were sieved to separate the roots from the soil, photographed, and dried following Cornelissen et al. (2003). Average values of dry root weight were used to describe the vertical root distribution as the root weight density provides a more accurate description of the root system (Satchithanantham et al., 2014). The roots can reach 140 cm depth, but ~75% is located above 70 cm depth.

2.3.5. Soil properties

Five soil samples were taken from the top 200 cm to determine soil physical properties (such as bulk density and the percentage of sand, silt and clay). The hydraulic properties of the soil were described with the van Genuchten–Mualem model (van Genuchten, 1980) without considering hysteresis and estimated using pedotransfer functions. The ROSETTA model (Schaap et al., 2001) was applied to determine the required soil hydraulic parameters (such as k_s, θ_r, and n) based on textural information and bulk density, which were calibrated afterwards.

2.3.6. Model calibration and validation

The model was first calibrated using the measured soil water content (about 40% of the total measurements) from May 2 to June 30, 2012. The model was validated with the remaining soil water data measured from July 1 to September 26, 2012. To reduce the number of parameters in the model calibration, the saturated soil water content (θ_s = 0.36 cm^3/cm^3) was fixed according to the measured soil water content in the saturated zone, while the pore connectivity was assumed to be 0.5 (Mualem, 1976). The Levenberg–Marquardt optimization (Marquardt, 1963) was used to match the observed data by adjusting the hydraulic parameters of the soil that were subsequently used for model validation. The coefficient of determination (r^2) and root mean square error (RMSE) were used to evaluate the model performance.

2.3.7. Soil water balance

To investigate the interaction between groundwater and plants, the soil water balance in the root zone (0–140 cm) was calculated by:

$$\frac{dS}{dt} = P_e - E_a - T_a - R - D \quad (10)$$

where dS/dt is the soil water storage change (cm/d), P_e is the effective precipitation (cm/d), E_a is the actual evaporation (cm/d), T_a is the actual transpiration (cm/d), D is the drainage from the root zone (cm/d), R is the surface runoff (cm/d). The negative values of D represent upward flux (G_{up}) consumed by T_a, whereas the positive values mean downward flux that can be regarded as groundwater recharge (G_r). G_{up} was only calculated for non-rainfall days as numerous studies found that tree water use is close to zero during rainy days (Qu et al., 2007 and Zhao and Liu, 2010). The surface runoff during the experiment can be neglected because there was no runoff observed. From the model results, D was calculated with Eq. (10) to analyze groundwater recharge or transpiration.

3. Results

3.1. Field and laboratory measurements

There were 39 rainy days between May and September 2012. The daily P_g varied between 0.1 and 50.6 mm with a mean of 7.6 mm. About 35.6% of rainfall was above 10 mm/d and contributed to roughly 77.5% of the total rainfall volume. The maximum monthly P_g occurred in July (141.7 mm) and the minimum in May (33.7 mm). The P_g pattern was sporadic with a high seasonal variation, similar to many other arid regions (Loik et al., 2004; Rappold, 2005 and Zhao and Liu, 2010). Using the measured P_g, the total canopy interception was calculated to be 76.6 mm by Eq. (5), accounting for 18.6% of the P_g, making it a significant component of the water balance.

The average soil bulk density was 1.50 g/cm^3. The top layer of 20 cm contained ~90% sand and 10% silt and was slightly finer than the underlying layers. The sand content below the top layer ranged between 98.5% and 99.4% and the silt content ranged between 0.6% and 1.5%. The soil profile was quite homogenous and therefore conceptualized as homogenous material in the flow modelling.

The average soil water content varied greatly (0.12–0.22) and was controlled by heavy rainfall and water table fluctuations (Fig. 2). It decreased from the beginning of the experiment with the decline in the water table until a heavy rainfall occurred in June and then dropped again. The lowest soil water content was 0.12 in the end of June when the cumulative rainfall was 136.2 mm and the water table was at the lowest level (Fig. 2). The soil water content increased dramatically after the continuous rainfall at the end of July, remaining at a relatively stable value of 0.20.

During the experiment, the water table depth varied from 113.6 to 166.4 cm, with a mean of 141.1 cm and a standard deviation of 16.1 cm (Fig. 2). It declined continuously at ~0.5 cm/d before June due to the evapotranspiration (ET). After a heavy rainfall event

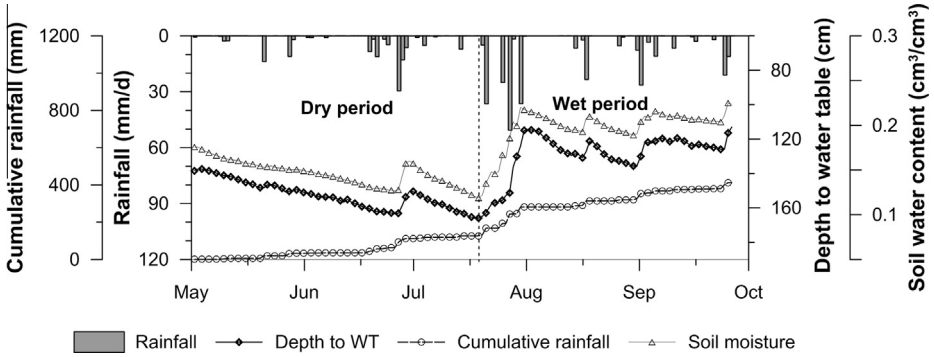

Fig. 2. Measured rainfall, water table depth, and average soil moisture in 2012.

Table 1
Calibrated soil hydraulic parameters.[a]

θ_r (cm^3/cm^3)	θ_s (cm^3/cm^3)	a (cm^{-1})	n	k_s (cm/d)	h_{50} (cm)
0.01	0.36	0.069	1.61	1178	−950

[a] θ_r, residual water content; θ_s, saturated water content; a, empirical constant; n, shape parameter; k_s, saturated hydraulic conductivity; h_{50}, pressure head at which transpiration is reduced by 50%.

(48.7 mm) at the end of June, the water table increased ~13.0 cm and then decreased until late July. From 20 to 30 July, the water table increased over 50.0 cm after the heaviest observed rainfall event (115.0 mm) and then fluctuated with rainfall. The response of the water table to rainfall was controlled by soil water conditions and rainfall intensity, with no reaction observed for rainfall below 10 mm/d. Above 10 mm/d, the water table reacted differently depending on the soil water content. For example, the water table increased only 0.2 cm after a rainfall of 11.1 mm on June 21 when the soil water content was lowest (mean of 0.16), while it raised 1.5 cm after a rainfall of 11.0 mm on May 25 (mean soil water content of 0.18).

The trend analysis of the cumulative rainfall, soil water content, and water table indicated a changing point on July 20. Before this, the average soil water content and water table depth were 0.15 and 97.6 cm, respectively, which changed to 0.20 and 122.3 cm, respectively after July 20. This divided the measurement period into a dry and wet period (Fig. 2).

3.2. Calibration and validation

The soil hydraulic parameters calibrated using the measured soil water content are shown in Table 1 and were similar to the values estimated using ROSETTA. The simulated soil water content and transpiration were not sensitive to h_{50}, consistently with previous studies (Skaggs et al., 2006 and Zhu et al., 2009). The measured and simulated soil water content at various depths are shown in Fig. 3. The over-predicted soil water content at 20 cm depth may be due to the presence of finer material, while its variations at 20–100 cm were well captured in the simulation. Below 100 cm, the rapid fluctuation of the groundwater during the high-level period (after August) caused bigger changes in the simulated soil water content than in the measured data. These short-term oscillations in soil water content close to the water table are difficult to reproduce in many cases (Forkutsa et al., 2009). Although there were small differences in certain layers, the agreement between the calculated and measured soil water contents was good (Fig. 3). The statistical indices describing the model performance during calibration and validation are listed in Table 2. As expected, the R^2 was slightly lower for the validation than for the calibration period. The overall RMSE between the measured and simulated soil water content was 0.005, with a coefficient of determination of 0.98, indicating a good agreement between the simulated and observed data.

3.3. Short-term simulation results

The components of soil water balance were calculated with Eq. (10) and are shown in Table 3. The daily temporal variation of the actual evaporation (E_a) was correlated to the soil water content with a correlation coefficient of 0.66 and the correlation analyses further indicated a higher E_a correlation coefficient with top soil water (0–80 cm) than with soil water below 80 cm. The average E_a was 0.15 cm/d in the dry period (May–June) when the mean soil water content was 0.15, increasing to 0.17 cm/d in the wet period (August–September) with an average soil water content of 0.21. The E_a/E_p ratio showed that E_a approaches E_p during rainy days (Fig. 4), with the longest period lasting for 5 days in the end of June after a heavy rainfall (~36.0 mm). Subsequently, the ratio dropped significantly due to the high seepage rate and low retention capacity of the sandy soil. The lowest ratio was close to zero in the driest period (late June–mid July), indicating a very dry soil.

Soil water storage change (dS/dt) was positively correlated with P_e with a correlation coefficient of 0.90, indicating precipitation as one of the major sources of soil water. During the low monthly rainfall in May and August, dS/dt was negative due to the consumption of E_a and actual transpiration (T_a). In contrast, dS/dt was positive under high rainfall in July and September. dS/dt also had a strong correlation with drainage (D) ($r = 0.64$), indicating the contribution from groundwater.

T_a increased from 0.20 cm/d in May to 0.27 cm/d in June, stayed relatively constant until August, and decreased to 0.12 cm/d in September (Table 3). The seasonal variation showed that T_a in the dry season (June) was comparable to the wet season (August), indicating the existence of unrestricted groundwater supply to T_a in addition to soil water. The T_a/T_p ratio was very close to 1.00 in the driest period (Fig. 4), providing additional evidence of groundwater use by plants. The positive monthly bottom flux indicated the groundwater contribution to T_a.

The results showed that groundwater uptake amounted to ~55% of tree transpiration during the dry period and 16–19% during the wet period (Table 4). The monthly groundwater recharge (G_r) was 0–3.7% of the gross rainfall in the dry period and 7–8% in the wet period (Table 4) and groundwater recharge only occurred after exceptionally heavy rainfall.

3.4. Isotope analysis

The isotopic compositions of rainwater, stem water, and soil water are shown in Fig. 5. The overall evaporation line had a slope of 5.5, which is lower than the slope of the local meteoric water (8.6) as shown in Fig. 5a, and therefore indicates the effect of evaporation in soil water. The isotopic values for soil water below 100 cm depth scatter around the local meteorological water line (LMWL), suggesting little or no evaporation of deep soil water. The majority of soil water above a depth of 100 cm was located below the LMWL due to kinetic enrichment (Fig. 5b), but some were laying on the LMWL. Those samples were taken during the wet period after the heaviest rainfall (end of July) and represent the isotopic signature of rainfall. The slope of the isotopic composition of stem water was 5.9, between deep (8.6) and shallow soil water (5.5), indicating that trees use both groundwater and soil water.

The average isotopic composition of $\delta^{18}O$ decreased from −4.8‰ at 20 cm depth to −7.0‰ at 80 cm depth, remaining then relatively constant and similar to groundwater (Fig. 5c). The variation of the average $\delta^{18}O$ above 80 cm was ~3.2‰, which is higher than the average of 0.8‰ below 80 cm depth, indicating strong evaporation in the top soil. To analyze the sources of tree water use, the IsoSource multiple-source isotopic mass balance model (Phillips and Gregg, 2003 and Phillips et al., 2005) was used to identify the water sources and their contributions. Based on the vertical variation of isotopic compositions from Fig. 5c, we selected sampling date when at least one sample at 0–40 cm, 60–80 cm, and 100–160 cm was collected (Fig. 6). The results indicated that groundwater contributed to 45% of plant water use on May 5, decreasing to 4–12% during the wet period, when trees mainly use shallow soil water. In contrast, the contribution from the 0 to 40 cm layer accounted for 65–86% during the wet period and only 34% during the dry period.

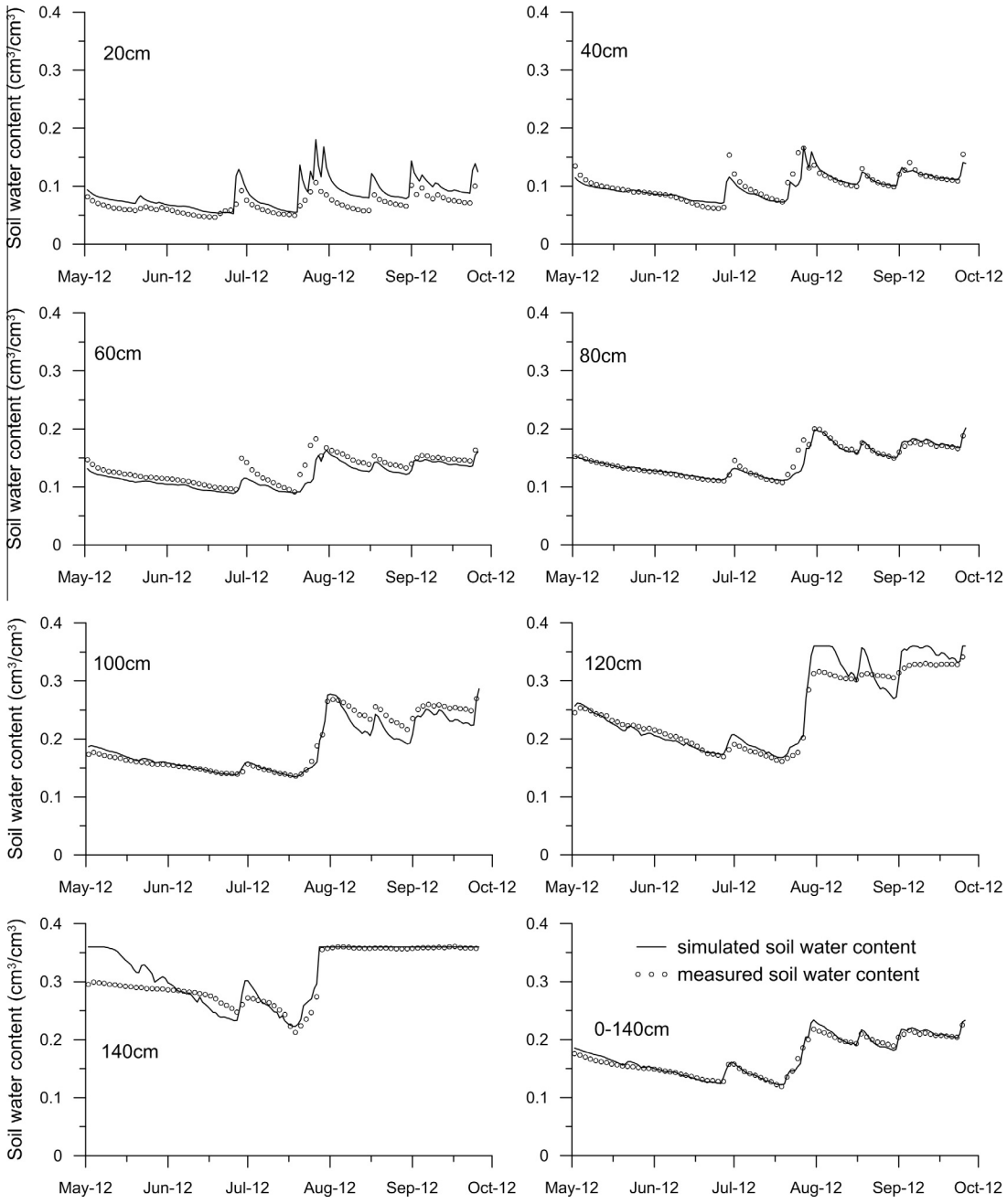

Fig. 3. Simulated and measured soil moisture at various depths.

Table 2
Root mean square error and coefficient of determination between observed and simulated soil water content.[b]

Soil layer (cm)	RMSE		R^2	
	Calibration	Validation	Calibration	Validation
20	0.015	0.026	0.77	0.81
40	0.009	0.010	0.96	0.77
60	0.011	0.016	0.86	0.77
80	0.003	0.009	0.96	0.88
100	0.006	0.017	0.98	0.94
120	0.007	0.025	0.94	0.94
140	0.035	0.009	0.79	0.64
0–140	0.005	0.005	0.98	0.98

[b] RMSE, root mean square error; r^2, coefficient of determination.

3.5. Long-term simulation

The results from the long-term simulation (1992–2010) are presented in Fig. 7. The mean annual potential ET varied insignificantly with a coefficient of variation of 0.06. Similarly, stable potential ET has been observed in other arid zones, such as Ethiopia (Tilahun, 2006). However, the annual precipitation varied significantly, ranging from 569 mm in 2001 to 248 mm in 2005 (Fig. 7a). The annual precipitation at 5% and 95% probability were 258 mm and 568 mm during 1953–2010, respectively, indicating that the variation of the annual precipitation for our selected period represented well the long-term features of the climate in the study area.

The highest precipitation usually occurred in July or August, with mean monthly values of 119 mm and 88 mm, respectively

Table 3
Monthly water balance values and mean soil water content.[c]

Month	P_e (cm/d)	E_a (cm/d)	T_a (cm/d)	D (cm/d)	dS/dt (cm/d)	Soil water content (cm^3/cm^3)
May	0.09	0.16	0.20	−0.13	−0.14	0.16
June	0.21	0.12	0.26	−0.23	0.06	0.14
July	0.47	0.18	0.27	−0.32	0.34	0.15
August	0.11	0.19	0.30	−0.13	−0.25	0.20
September	0.23	0.15	0.12	−0.29	0.24	0.21

[c] P_e, effective precipitation; E_a, actual evaporation; T_a, actual transpiration; D, bottom flux; dS/dt, soil water storage change.

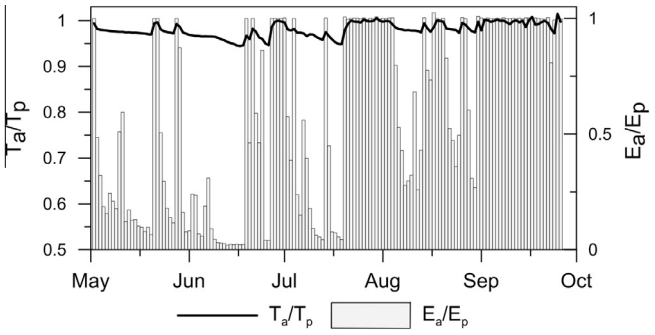

Fig. 4. Ratio between actual (T_a) and potential transpiration (T_p) (black line) and actual (E_a) and potential evaporation (E_p) (bars).

(Fig. 7a). The water table generally declined before July and increased in response to rainfall, with annual variation of less than 50 cm. An exception occurred in 2007, with a variation of 240 cm (Fig. 7a). This might have been due to the increase in groundwater pumping for irrigation in 2007 after a 2-year consecutive drought (2005–2006). The range of the mean annual water table variation over the long-term period, excluding 2007, was only 79 cm.

The T_a/T_p ratio was lowest in 2007 (0.78) and ranged between 0.91 and 1.00 in the other years (Fig. 7b). When the water table was less than 140 cm depth, T_a almost equaled T_p (Fig. 8a) with no relation with the annual precipitation, suggesting that trees did not suffer water stress even for the driest year because of constant groundwater supply. With the increase in ET_p/P_g, T_p/P_g increased linearly (Fig. 8b), also indicating an unlimited water source for T_a. The T_a/T_p ratio decreased slightly with the water table drop from 140 to 180 cm depth. However, tree water use will drop dramatically with a water table depth below 180 cm due to human activities (as in 2007) (Fig. 8a). The relation between the water table depth and T_a suggested a critical depth of 180 cm below which the willow trees will suffer from water stress in the site (see Fig. 8a).

The E_a/E_p ratio ranged between 0.30 and 1.00 with a mean of 0.66, and was controlled by the annual precipitation and water table depth (Fig. 7b). When the water table depth was less than 90 cm, the E_a/E_p ratio was close to 1.00, as in 1996, 2003, and 2004. This means that soil evaporation consumes a large amount of groundwater when the water table is shallow, which is consistent with the soil evaporation extinction depth of ~80 to 100 cm derived from the isotopic analysis. The exception was 1997 when the water table depth was 90 cm and the ratio was only 0.79 due to a low annual precipitation of 316 mm (~1/3 lower than the long-term mean). The impact of annual precipitation on soil evaporation was more significant when the water table dropped. For example, the water table was much deeper in 2007 (149 cm) than in 2006 (205 cm) but E_a/E_p was lower in 2006 (0.30) when the annual precipitation was 313 mm, in contrast with 2007 (0.49) with an annual precipitation of 439 mm.

Table 4
Groundwater uptake and recharge.[d]

Month	G_{up} (cm)	T_a (cm)	G_{up}/T_p (%)	G_r (cm)	P (cm)	G_r/P (%)
May	2.89	5.30	55	0.15	4.02	3.70
June	3.36	6.05	56	0.00	7.91	0.00
July	3.28	6.21	53	0.52	16.92	3.07
August	1.12	5.88	19	0.37	4.59	8.06
September	0.39	2.39	16	0.37	5.20	7.11

[d] G_{up}, Groundwater uptake; T_p, potential transpiration; G_r, groundwater recharge; P, precipitation.

3.6. Scenario simulation

A deep water table was assumed in the scenario simulation to represent impacts of groundwater abstraction. Under this condition, T_a and E_a decreased significantly (Fig. 9). The E_a/E_p ratio varied between 0.12 (1997) and 0.31(2002) with a mean of 0.21, while the T_a/T_p ratio ranged from 0.09 (1997) to 0.40 (2002) with a mean of 0.22. Comparing to the natural variation condition, the mean T_a/T_p decreased from 0.96 to 0.22 and the mean E_a/E_p decreased from 0.66 to 0.21, indicating that the drop in the water table had more impact on T_a than E_a. The correlation coefficient between T_a and the annual precipitation was 0.77, and 0.85 between E_a and the annual precipitation, indicating that the variation of T_a/T_p and E_a/E_p was controlled by the annual precipitation when water table was deep. The lower T_a and more dependent on precipitation in the deep-water condition indicate that vegetation will change from groundwater-dependent to precipitation-dependent. Due to less reliance on the constant groundwater source, the coefficient of variation of T_a/T_p increased from 5% for the natural condition to 38% for the scenario condition.

4. Discussion

4.1. Interaction between plants and groundwater

Rainfall had a large intra- and inter-annual variability at the study site (Figs. 1 and 7a), as recognized and observed in many arid regions (Tilahun, 2006 and Yaseef et al., 2009), with maximum to minimum annual rainfall ratios usually over 3 (FAO, 1989). As a response to rainfall variation, soil water also changes significantly with time (He et al., 2012), specially for shallow depths as observed in Fig. 3. However, the water table depth did not change significantly in comparison to the soil water (Figs. 1 and 3). Groundwater, therefore, provided a reliable water source for plants, being important for trees as shown in our study (Table 4), particularly during dry periods. We also found similar reports in other studies (Dawson and Pate, 1996; Cui and Shao, 2005; Naumburg et al., 2005 and Zhu et al., 2009). For example In Australia, *Banksia prionotes* derives the majority of its water from deeper sources during the dry season while, in the wet season, most of the water used derives from the upper soil layers being supplied by lateral roots (Dawson and Pate, 1996). In the Badanjilin desert in China, *P. euphratica* obtains 53% of its water

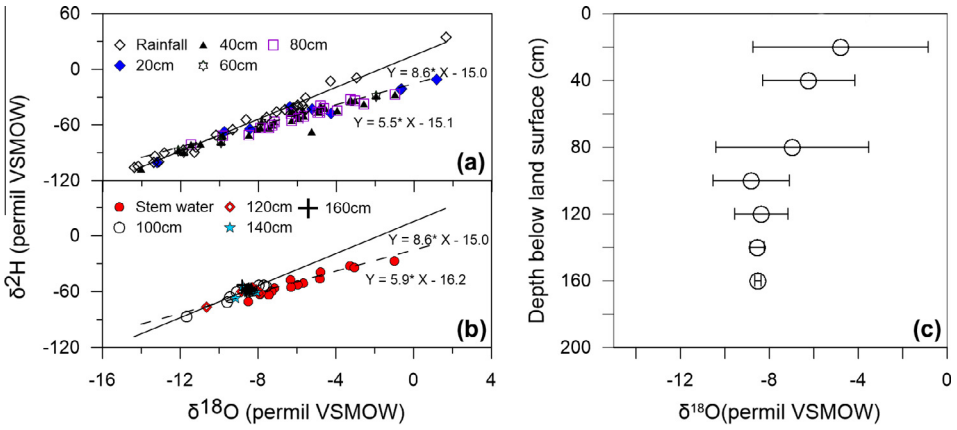

Fig. 5. Isotopic compositions of stem and soil water (a and b), and the variation of the mean isotopic composition with depth (c).

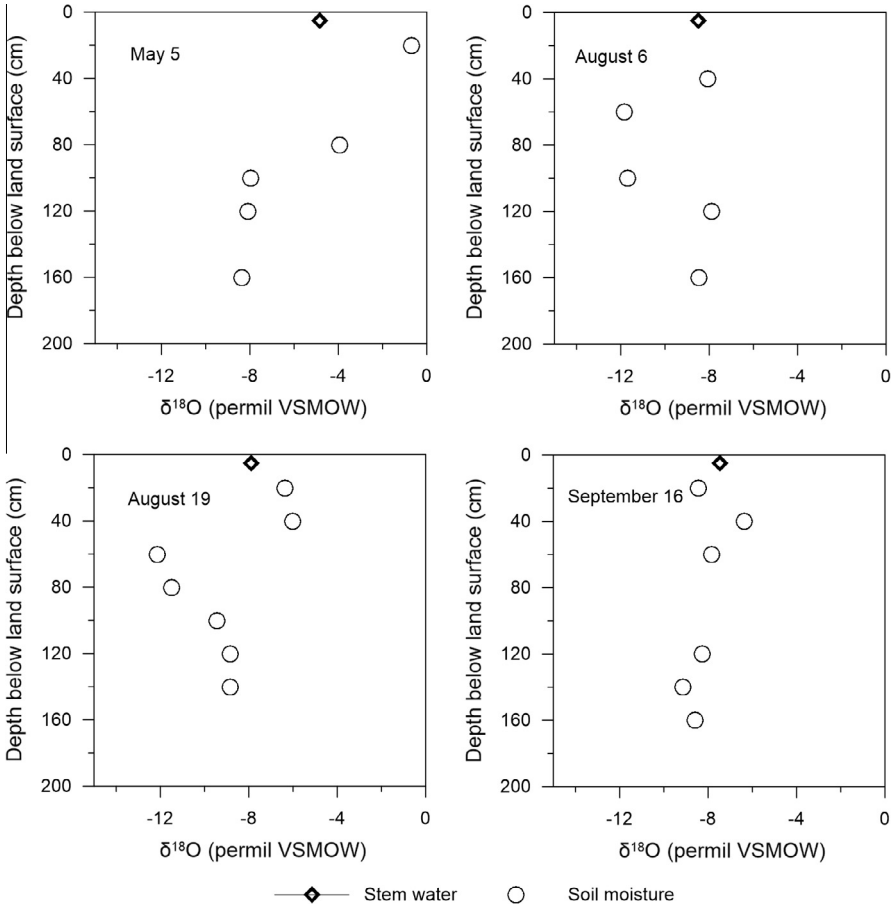

Fig. 6. Isotopic compositions of stem and soil water for selected days.

from groundwater (Zhu et al., 2009), while in the dry summer from central Portugal, groundwater uptake accounts for 73.2% of *Quercus suber* needs (Pinto et al., 2014).

It is recognized that trees can substantially reduce groundwater recharge. The global analysis of groundwater recharge and vegetation revealed that the latter is the second factor affecting groundwater recharge, following water input (Kim and Jackson, 2012). Groundwater recharge is reduced by vegetation through canopy interception and transpiration from soil water (Keese et al., 2005 and Scanlon et al., 2002). Canopy interception cannot be neglected, as shown in this study, as trees have a strong coupling between the canopy and the atmosphere, resulting in high evaporation rates from the wet canopy (Lankreijer et al., 1993). The effective precipitation is then reduced and groundwater recharge decreases as a result. Given the consumption of soil water by trees, soil water content is generally low in planted forests (Mu et al., 2003). Five-year water balance measurements by auto-weighting lysimeters suggested that soil water storage in the vegetated lysimeter was only 47% of the observed for a bare lysimeter (Wang et al., 2004). In addition, the long-term soil water accumulation was significantly greater in the upper 125 cm of a non-vegetated profile than for a vegetated soil in the Mojave Desert, Nevada (Gee et al.,

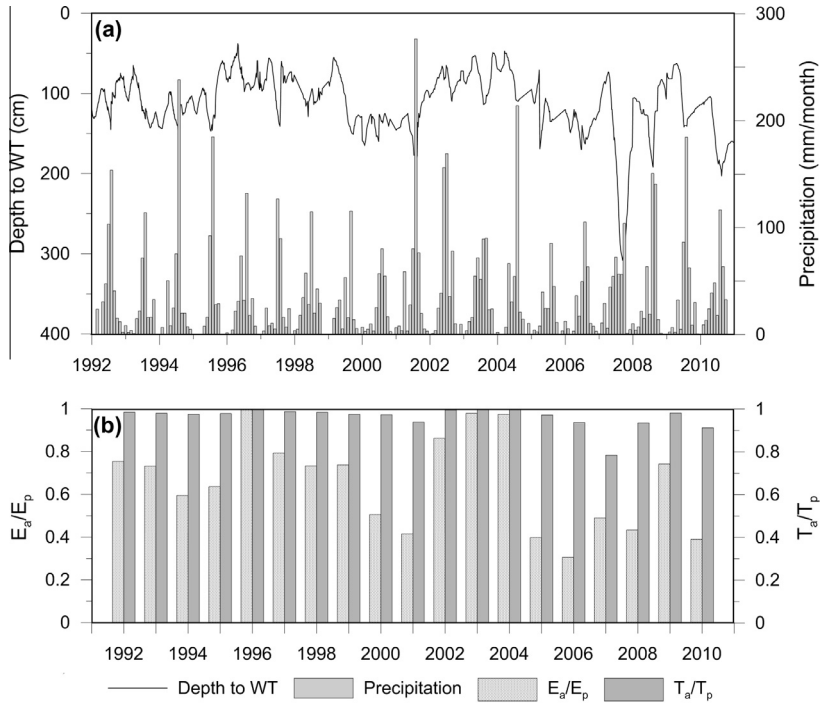

Fig. 7. Long-term water table and monthly precipitation (a) and ratios of actual (E_a) and potential evaporation (E_p) and actual (T_a) and potential transpiration (T_p) for the long-term simulation (b).

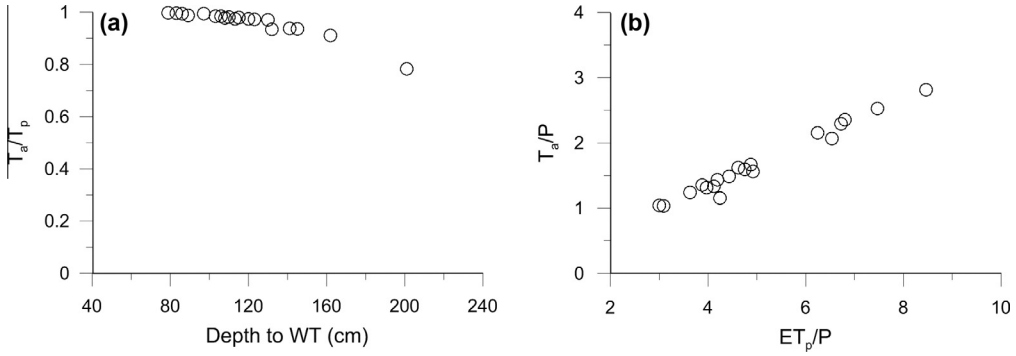

Fig. 8. The variation of the actual transpiration (T_a)/potential transpiration (T_p) ratio with water table depth (a) and relation between potential evapotranspiration (ET_p)/effective precipitation (P) ratio and T_a/P (b).

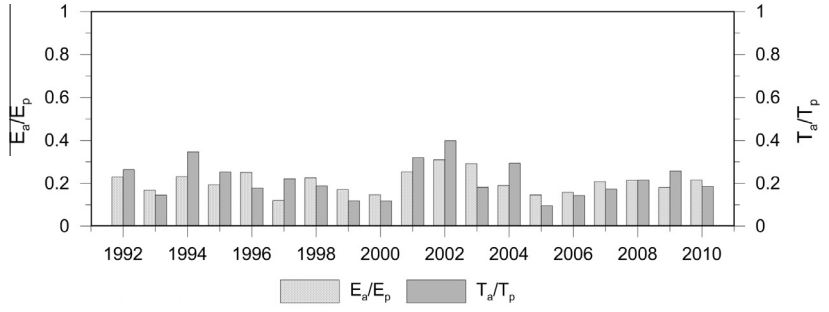

Fig. 9. Ratios of actual (E_a) and potential evaporation (E_p) and actual (T_a) and potential transpiration (T_p) for the scenario simulation.

1994; Andraski, 1997). As a result of canopy interception and consumption of soil water, groundwater recharge in forests is much lower than in other areas, such as bare soil, cropland, and grassland (Kim and Jackson, 2012). Therefore, the water table would drop in response to the reduced recharge. In Western Australia, the water table declined up to 550 cm following the plantation of millions of trees for dryland salinity management, with a more obvious drop in perched, local, and intermediate aquifers (George et al., 1999). However, tree plantings can have limited hydrological impacts if strategically placed in a catchment shown in a simulation study

(Cheng et al., 2014). The previous studies show that lower density of plantation will have less impact on groundwater availability (Horner et al., 2009 and Cheng et al., 2014).

A severe drop of water table caused by the groundwater recharge reduction will affect the growth of trees as show in Fig. 8 and some may die off as observed by Bacchus (1997). Afforestation is carried out in many arid regions to alleviate land degradation, reduce poverty, and improve livelihood (FAO, 2010 and Cao, 2011). However, this study and the cases mentioned in the above discussion indicate that ecological restoration in arid zone should be cautious of over-planting of tree that may induce quick drop of water table beyond the critical depth, which in turn may result in the death of planted trees that are groundwater-dependent. A proper selection of tree species for afforestation in water-limited areas may reduce the risk (Cao et al., 2010). For example, native plants usually have lower water requirements than invasive or artificially planted trees (Cavaleri and Sack, 2010), which supports the simple rehabilitation of natural ecosystems of high water efficiency to maintain sustainable ecosystems (Zhou et al., 2013).

4.2. Climate variations and anthropogenic impact on trees

T_a/T_p (Figs. 4 and 7b) was still very high even for very dry seasons or years, suggesting that trees are adapted to the local variation of climate. One important adaptation mechanism is the specific root pattern, including shallow lateral and deep roots that allow the search for water (Lubczynski, 2009). The shallow roots absorb soil water provided by precipitation, while the deep roots take up groundwater (Batanouny, 2001), which is particularly vital in dry years, when the shallow roots cannot get enough water from the top soil to maintain tree growth (Goldstein et al., 2008). Therefore, the development of deep roots by trees in arid regions, up to a maximum of 9.5 ± 2.4 m is common, in comparison with the global average value of 4.6 ± 0.5 m (Canadell et al., 1996). When the water table falls over dry periods, roots will grow to maintain water access throughout the growing season, with substantial volumes of groundwater being used. Canham et al. (2012) used root in-growth bags to study the dynamics of root grow of *Banksia* under a naturally fluctuating water table and found that roots grew above the water table in all seasons. The ability of root growth is vital to maintain the access to groundwater in dry seasons. Kranjcec et al. (1998) used rhizoponds to investigate the root growth of North American cottonwood species under different controlled rates of water table decline and also found that root growth was promoted by water table decline. Although the mass of deep roots is relatively small, as shown in this study, water uptake can be up to 60% of the total water use by plants as deep roots can access more stable water sources (Canadell et al., 1996). The short- and long-term simulation as well as the analysis of root pattern and response to water table decline indicate that the climatic variation itself may not have severe negative impact on trees.

Nevertheless, the drop in the water table caused by anthropogenic activities is larger than the natural fluctuations due to climate variability (Fig. 7a), and further aggravated by climate change (Kløve et al., 2013). If the drop is faster than the growth rate of deep roots, transpiration will decrease dramatically (this study, Luo and Sophocleous, 2010 and Soylu et al., 2011). Further simulation studies have revealed an exponential decay in transpiration with water table depth (Shah et al., 2007 and Luo and Sophocleous, 2010) and transpiration of *P. euphratica*, for example, will reduce by 74% with a decrease in the water table depth from 2 to 3 m (Zhu et al., 2009). The laboratory tests using rhizopods also indicate that a rapid groundwater table decline results in a severe impact on plant growth (Mahoney and Rood, 1992; Kranjcec et al., 1998 and Guilloy et al., 2011). A short-terming monitoring on the response of *Populus deltoids* to water table drop shows that shoot water potential decreases and then leaf mortality occurs (Cooper et al., 2003). Long-term monitoring (over decades) indicate that higher rate of groundwater drawdown will result in the mortality of forests or the transition to an alternative ecohydrological state. Besides the small scale studies mentioned above, regional monitoring also indicates that groundwater decline negatively affects groundwater-dependent plants (Stromberg et al., 1996; Cooper et al., 2006; Elmore et al., 2006; Cunningham et al., 2011; Barron et al., 2014; Kath et al., 2014 and Sommer and Froend, 2014). For example, lowering water table reduced groundwater contribution to plant water use by 62% in the San Luis Valley, Colorado, USA (Copper et al., 2006). In the Condamine catchment, Queensland, Australia, Canopy condition of *Eucalyptus camaldulensis* and *Eucalyptus populnea* declined abruptly when water table is lowered beyond a certain depth (Kath et al., 2014).

4.3. Limitation and generalization of the study

In this study, root growth was ignored. Under natural conditions, the variation of the water table is usually less than 0.5 m and root growth can be ignored. In our scenario conditions, the water table decline may be too fast for root elongation, so that the roots lose contact with the water table and growth decreases due to water stress, as observed in previous experiments (Mahoney and Rood, 1992 and Kranjcec et al., 1998). Even though, not including root growth will underestimate the groundwater contribution to plant water use to some extent (Imada et al., 2008) and our results can be considered conservative. We also ignored hydraulic redistribution that the passive movement of water between different soil parts via plant root systems (Prieto et al., 2012; David et al., 2013 and Gou and Miller, 2014) and this process may play a significantly role when water table is deep.

The general conclusions of the study are applied to phreatophytes in arid/semi-arid regions, including trees, bushes and herbs as observed by Elmore et al. (2006). The results are particularly valid to trees in shallow groundwater regions that usually occur in the discharge areas of groundwater flow systems (Tóth, 1963), such as riparian zones. However, we should note that the quantitative conclusions, such as the contribution of groundwater to transpiration and transpiration reduction after water table decline are site-specific. Generally speaking, phreatophytes are dependent more on groundwater and have significant response to water table decline in drier climate; fine textured soils will benefit the survival of phreatophytes when water table declines caused by groundwater abstraction as they have larger capillary rise; native trees are less sensitive to water table decline as they have higher efficiency of water use.

5. Conclusions

In this study, the HRDRUS-1D model and stable isotopes were used to study the groundwater contribution to willow trees and the groundwater recharge in an arid experiment site for a short-term (May 2 to September 26, 2012) and long-term period (1992–2010). The short-term simulation was divided into a dry and wet period. In the dry season, transpiration was comparable to the wet season and T_a/T_p was close to 1 during the entire growing season, indicating the use of groundwater by trees. The groundwater contribution to the tree transpiration amounted to ~55% during the dry period and 16–19% during the wet period based on the modeling results and confirmed by the stable isotope study. Groundwater recharge occurred occasionally after heavy rainfall, corresponding to 3–8% of total rainfall. This reduction in recharge resulted from canopy interception and consumption of soil water

by trees, which in turn will affect tree growth as they heavily rely on groundwater. Therefore, a proper selection of tree species for afforestation is critical in water-limited areas, to avoid an increase in water shortage and weakening of the ecological function of trees. Therefore, the recreation of natural environments characterized by high water efficiency is recommended, to have sustainable ecosystems.

In the long-term simulation, T_a/T_p ranged between 0.91 and 1.00 except in 2007 when the water table dropped dramatically due to human activity. The relatively high T_a/T_p indicated that trees adapt to local environmental conditions by developing shallow lateral and deep roots to use soil and groundwater, respectively. Deep roots, in particular, play a vital role in dry seasons by absorbing groundwater. Therefore, climatic variation itself may not seriously affect trees in arid zones. However, significant changes in the water table due to anthropogenic activities, decreased transpiration dramatically.

Acknowledgments

The authors thank Prof. Li Yan at Xinjiang Institute of Ecology and Geography of Chinese Academy of Science for the comments on the manuscript. The critical review of the associate editor and two anonymous referees was very useful for the further improvement of the manuscript. The research was funded by Ecohydrological Survey in the Hailiutu River Basin (12120113104100), China National Natural Science Foundation (41472228) and Key laboratory of groundwater and ecology in arid regions of China Geological Survey. A research grant was awarded to the first author to prepare the manuscript at UNESCO-IHE by the Honour Power Foundation.

References

Allen, R.G., Pereira, L.S., Raes, D., Smith, M., 1998. Crop Evapotranspiration: Guidelines for Computing Crop Water Requirements. FAO Irrigation and Drainage Paper, Rome, 56.

Andraski, B.J., 1997. Soil-water movement under natural-site and waste-site conditions: a multiple-year field study in the Mojave Desert, Nevada. Water Resour. Res. 33 (8), 1901–1916.

Asbjornsen, H., Goldsmith, G.R., Alvarado-Barrientos, M.S., Rebel, K., Van Osch, P.F., Rietkerk, M., Chen, J., Gotsch, S., Tobón, C., Geissert, D.R., Gómez-Tagle, A., Vache, K., Dawson, T.E., 2011. Ecohydrological advances and applications in plant–water relations research: a review. J. Plant Ecol. 4 (1–2), 3–22.

Bacchus, S.T., 1997. Premature decline and death of trees associated with a man-made lake and groundwater withdrawals in Albany, Georgia. In: Proceedings of the 1997 Georgia Water Resources Conferences, Athens, Georgia.

Barbeta, A., Mejia-Chang, M., Ogaya, R., Voltas, J., Dawson, T.E., Penuelas, J., 2015. The combined effects of a long-term experimental drought and an extreme drought on the use of plant-water sources in a Mediterranean forest. Glob. Change Biol. 21, 1213–1225.

Barron, O., Froend, R., Hodgson, G., Ali, R., Dawes, W., Davies, P., McFarlane, D., 2014. Projected risks to groundwater-dependent terrestrial vegetation caused by changing climate and groundwater abstraction in the Central Perth Basin, Western Australia. Hydrol. Process. 28 (22), 5513–5529.

Batanouny, K.H., 2001. Plants in the Desert of the Middle East. Springer Berlag, Heidelberg.

Bian, Z., Lei, S., Inyang, H.I., Chang, L., Zhang, R., Zhou, C., He, X., 2009. Integrated method of RS and GPR for monitoring the changes in the soil moisture and groundwater environment due to underground coal mining. Environ. Geol. 57 (1), 131–142.

Blom, G., 1958. Statistical Estimates and Transformed Beta Variables. John Wiley and Sons, New York.

Brooks, R.H., Corey, A.T., 1966. Properties of porous media affecting fluid flow. J. Irrig. Drain. Div. Am. Soc. Civ. Eng. 92 (IR2), 61–88.

Bulter, J.J., Kluitenberg, G.J., Whittemore, D.O., Loheide II, S.P., Jin, W., Billinger, M.A., Zhan, X., 2007. A field investigation of phreatophyte-induced fluctuations in the watertable. Water Resour. Res. 43 (2). http://dx.doi.org/10.1029/2005WR004627.

Canadell, J., Jackson, R.B., Ehleringer, J.R., Mooney, H.A., Sala, O.E.T., Schultze, E.T.D., 1996. Maximum rooting depth of vegetation types at the global scale. Oecologia 108, 583–595.

Canham, C.A., Froend, R.H., Stock, W.D., Davies, M., 2012. Dynamics of phreatophyte root growth relative to a seasonally fluctuating water table in a Mediterranean-type environment. Oecologia 170, 909–916.

Cao, S., 2011. Impact of China's large-scale ecological restoration program on the environment and society in arid and semiarid areas of China: achievements, problems, synthesis, and application. Environ. Sci. Technol. 43, 317–335.

Cao, S., Wang, G., Chen, L., 2010. Questionable value of planting thirsty trees in dry regions. Nature 465, 31.

Cavaleri, M.A., Sack, L., 2010. Comparative water use of native and invasive plants at multiple scales: a global meta-analysis. Ecology 91, 2705–2715.

Cheng, X., Benke, K.K., Beverly, C., Christy, B., Weeks, A., Barlow, K., Reid, M., 2014. Balancing trade-off issues in land use change and the impact on streamflow and salinity management. Hydrol. Process. 28, 1641–1662.

Cheng, X., Hung, M., Shao, M., Yu, M., 2009. Canopy interception of tree and shrub plantations in a farming-pastoral zone of Loess Plateau. Chin. J. Ecol. 28 (7), 1213–1217 (in Chinese with English abstract).

Cooper, D.J., D'Amico, D.R., Scott, M.L., 2003. Physiological and morphological response patterns of *Populus deltoides* to alluvial groundwater. Environ. Manage. 31 (2), 215–226.

Cooper, D.J., Sanderson, J.S., Stannard, D.I., Groeneveld, D.P., 2006. Effects of long-term water table drawdown on evapotranspiration and vegetation in an arid region phreatophyte community. J. Hydrol. 325, 21–34.

Cornelissen, J.H.C., Lavorel, S., Garnie, R.E., Diaz, S., Buchmann, N., Gurvich, D.E., Reich, P.B., ter Steege, H., Morgan, H.D., van der Heijden, M.G.A., Pausas, J.G., Poorter, H., 2003. A handbook of protocols for standardized and easy measurement of plant functional traits worldwide. Aust. J. Bot. 51 (4), 335–380.

Costelloe, J.F., Payne, E., Woodrow, I.E., Irvine, E.C., Western, A.W., Leaney, F.W., 2008. Water sources assessed by arid zone riparian trees in highly saline environments, Australia. Oecologia 156, 43–52.

Cui, Y.L., Shao, J.L., 2005. The role of ground water in arid/semiarid ecosystems, Northwest China. Ground Water 43, 471–477.

Cunningham, S.C., Thomson, J.R., Mac Nally, R., Read, J., Baker, P.J., 2011. Groundwater change forecasts widespread forest dieback across an extensive floodplain system. Freshwater Biol. 56, 1494–1508.

David, T.S., Henriques, M.O., Kurz-Besson, C., Nunes, J., Valente, F., Vaz, M., Pereira, J.S., Siegwolf, R., Chaves, M.M., Gazarini, L.C., David, J.S., 2007. Water-use strategies in two co-occurring Mediterranean evergreen oaks: surviving the summer drought. Tree Physiol. 27, 793–803.

David, T.S., Pinto, C.A., Nadezhdina, N., Kurz-Besson, C., Henriques, M.O., Quilhó, T., Čermák, J., Chaves, M.M., Pereira, J.S., David, J.S., 2013. Root functioning, tree water use and hydraulic redistribution in *Quercus suber* trees: a modeling approach based on root sap flow. For. Ecol. Manage. 307, 136–146.

Dawson, T.E., Pate, J.S., 1996. Seasonal water uptake and movement in root systems of Australian phraeatophytic plants of dimorphic root morphology. Oecologia 107 (1), 13–20.

Elmore, A.J., Manning, S.J., Mustard, J.F., Craine, J.M., 2006. Decline in alkali meadow vegetation cover in California: the effects of groundwater extraction and drought. J. Appl. Ecol. 43, 770–779.

FAO, 1989. Arid zone forestry: a guide for field technicians. FAO Conservation Guide No. 20, Rome, Italy.

FAO, 2010. Global forest resources assessment 2010 – main report. FAO Forestry Paper No. 140, Rome, Italy.

Farrington, P., Bartle, G.A., 1991. Recharge beneath a Banksia woodland and a *Pinus pinaster* plantation on coastal deep sands in south Western Australia. For. Ecol. Manage. 40, 101–118.

Forkutsa, I., Sommer, R., Shirokova, Y.I., Lamers, J.P.A., Kienzler, K., Tischbein, B., Martius, C., Vlek, P.L.G., 2009. Modeling irrigated cotton with shallow groundwater in the Aral Sea Basin of Uzbekistan: I. Water dynamics. Irrig. Sci. 27, 331–346.

Gee, G.W., Wierenga, P.J., Andraski, B.J., Young, M.H., Fayer, M.J., Rockhold, M.L., 1994. Variations in water balance and recharge potential at three western desert sites. Soil Sci. Soc. Am. J. 58, 63–72.

George, R.J., Nulsen, R.A., Ferdowsian, R., Raper, G.P., 1999. Interactions between trees and groundwaters in recharge and discharge areas–a survey of Western Australian sites. Agric. Water Manage. 39, 91–113.

Goldstein, G., Meinzer, F.C., Bucci, S.J., Scholz, F.G., Franco, A.C., Hoffmann, W.A., 2008. Water economy of Neotropical savanna trees: six paradigms revisited. Tree Physiol. 28, 395–404.

Gou, S., Miller, G., 2014. A groundwater–soil–plant– atmosphere continuum approach for modelling water stress, uptake, and hydraulic redistribution in phreatophytic vegetation. Ecohydrology 7, 1029–1041.

Gribovszki, Z., Szilágyi, J., Kalicz, P., 2010. Diurnal fluctuations in shallow groundwater levels and streamflow rates and their interpretation – a review. J. Hydrol. 385, 371–383.

Guilloy, H., Gonzalez, E., Muller, E., Hughes, F.M.R., Barsoum, N., 2011. Abrupt drops in water table level influence the development of *Populus nigra* and *Salix alba* seedlings of different ages. Wetlands 31, 1249–1261.

He, Z., Zhao, W., Liu, H., Chang, X., 2012. The response of soil moisture to rainfall event size in subalpine grassland and meadows in a semi-arid mountain range: a case study in northwestern China's Qilian Mountains. J. Hydrol. 420–421, 183–190.

Horner, G.J., Baker, P.J., Mac Nally, R., Cunningham, S.C., Thomson, J.R., Hamilton, F., 2009. Mortality of developing floodplain forests subjected to a drying climate and water extraction. Glob. Change Biol. 15, 2176–2186.

Ibrahimi, M.H., Miyazaki, T., Nishimura, T., Imoto, H., 2013. Contribution of shallow groundwater rapid fluctuation to soil salinization under arid and semiarid climate. Arab J. Geosci. 7 (9), 3901–3911.

Imada, S., Yamanaka, N., Tamai, S., 2008. Water table depth affects *Populus alba* fine root growth and whole plant biomass. Funct. Ecol. 22, 1018–1026.

Karimov, A.K., Šimůnek, J., Hanjra, M.A., Avliyakulov, M., Forkutsa, I., 2014. Effects of the shallow water table on water use of winter wheat and ecosystem health: Implications for unlocking the potential of groundwater in the Fergana Valley (Central Asia). Agric. Water Manage. 131, 57–69.
Kath, J., Reardon-Smith, K., Le Brocque, A.F., Dyer, F.J., Dafny, E., Fritz, L., Batterham, M., 2014. Groundwater decline and tree change in floodplain landscapes: identifying non-linear threshold responses in canopy condition. Glob. Ecol. Conserv. 2, 148–160.
Keese, K.E., Scanlon, B.R., Reedy, R.C., 2005. Assessing controls on diffuse groundwater recharge using unsaturated flow modeling. Water Resour. Res. 41, 1–12.
Kelleners, T.J., Soppe, R.W.O., Ayars, J.E., Šimůnek, J., Skaggs, T.H., 2005. Inverse analysis of upward water flow in a groundwater table lysimeter. Vadose Zone J. 4, 558–572.
Kim, J.H., Jackson, R.B., 2012. A global analysis of groundwater recharge for vegetation, climate and soil. Vadose Zone J. 11 (1). http://dx.doi.org/10.2136/vzj2011.0021RA.
Kløve, B., Ala-Aho, P., Bertrand, G., Gurdak, J.J., Kupfersberger, H., værner, J.K., Muotka, T., Mykrä, H., Preda, E., Rossi, P., Uvo, C.B., Velasco, E., Pulido-Velazquez, M., 2013. Climate change impacts on groundwater and dependent ecosystems. J. Hydrol. 518, 250–266.
Kranjcec, J., Mahoney, J.M., Rood, S.B., 1998. The responses of three riparian cottonwood species to water table decline. Forest Ecol. Manage. 110, 77–87.
Lankreijer, H.J.M., Hendriks, M.J., Klaassen, W., 1993. A comparison of models simulating rainfall interception of forests. Agric. Forest Meteorol. 64, 187–199.
Leyer, I., 2005. Predicting plant species responses to river regulation: the role of water level fluctuations. J. Appl. Ecol. 42, 239–250.
Loik, M.E., Breshears, D.D., Lauenroth, W.K., Belnap, J., 2004. A multiscale perspective of water pulses in dryland ecosystems: climatology and ecohydrology of the western USA. Oecologia 141 (2), 269–281.
Lu, X., Jin, M., van Genuchten, M.T., Wang, B., 2011. Groundwater recharge at five representative sites in the Hebei Plain, China. Ground Water 49 (2), 286–294.
Lubczynski, M.W., 2009. The hydrogeological role of trees in water-limited environments. Hydrogeol. J. 17, 247–259.
Luo, Y., Sophocleous, M., 2010. Seasonal groundwater contribution to crop-water use assessed with lysimeter observations and model simulations. J. Hydrol. 389, 325–335.
Mahoney, J.M., Rood, S.B., 1992. Response of a hybrid poplar to water table decline in different substrates. Forest Ecol. Manage. 54, 141–156.
Maitre, D.C.L., Scott, D.F., Colvin, C., 1999. A review of information on interactions between vegetation and groundwater. Water SA 25 (2), 137–152.
Malagnoux, M., Sène, E.H., Atzmon, N., 2007. Forests, trees and water in arid lands: a delicate balance. Unasylva 58, 24–29.
Marquardt, D.W., 1963. An algorithm for least squares estimation of non-linear parameters. J. Ind. Appl. Math. 11, 431–441.
McCole, A.A., Stern, L.A., 2007. Seasonal water use patterns of *Juniperus ashei* on the Edwards Plateau, Texas, based on stable isotopes in water. J. Hydrol. 342, 238–248.
Mu, X., Xu, X., Wang, W., Wen, Z., Du, F., 2003. Impact of artificial forestry on soil moisture of the deep soil layer on Loess Plateau. Acta Pedol. Sin. 40, 210–217.
Mualem, Y., 1976. A new model for predicting the hydraulic conductivity of unsaturated porous media. Water Resour. Res. 25 (3), 385–396.
Naumburg, E., Mata-Gonzalez, R., Hunter, R.G., Mclendon, T., Martin, D.W., 2005. Phreatophytic vegetation and groundwater fluctuations: a review of current research and application of ecosystem response modeling with an emphasis on Great Basin vegetation. Environ. Manage. 35, 726–740.
Obakeng, T.O., 2007. Soil moisture dynamics and evapotranspiration at the fringe of the Botswana Kalahari with emphasis on deep rooting vegetation. PhD Thesis, Library of ITC, Enschede, The Netherlands.
Phillips, D.L., Gregg, J.W., 2001. Uncertainty in source partitioning using stable isotopes. Oecologia 127, 171–179.
Phillips, D.L., Gregg, J.W., 2003. Source partitioning using stable isotopes: coping with too many sources. Ecosyst. Ecol. 136, 261–269.
Phillips, D.L., Newsome, S.D., Gregg, J.W., 2005. Combining sources in stable isotope mixing models: alternative methods. Oecologia 144, 520–527.
Pinto, C.A., Nadezhdina, N., David, J.S., Kurz-Besson, C., Caldeira, M.C., Henriques, M.O., Monterio, F.G., Pereira, J.S., David, T.S., 2014. Transpiration in *Quercus suber* trees under shallow water table conditions: the role of soil and groundwater. Hydrol. Process. 28 (25), 6067–6079.
Prieto, I., Armas, C., Pugnaire, F.I., 2012. Water release through plant roots: new insights into its consequences at the plant and ecosystem level. New Phytol. 193, 830–841.
Qu, Y.P., Kang, S.Z., Li, F.S., Zhang, J.H., Xia, G.M., Li, W.C., 2007. Xylemsap flows of irrigated *Tamarix elongata* Ledeb and the influence of environmental factors in the desert region of Northwest China. Hydrol. Process. 21, 1363–1369.
Rappold, G.D., 2005. Precipitation analysis and agricultural water availability in the Southern Highlands of Yemen. Hydrol. Process. 19 (2), 2437–2449.
Richard, A., Galle, S., Descloitres, M., Cohard, J.M., Vandervaere, J.P., Séguis, L., Peugeot, C., 2013. Interplay of riparian forest and groundwater in the hillslope hydrology of Sudanian West Africa (northern Benin). Hydrol. Earth Syst. Sci. 17, 5079–5096.
Satchithanantham, S., Krahn, V., Sri Ranjan, R., Sager, S., 2014. Shallow groundwater uptake and irrigation water redistribution within the potato root zone. Shallow groundwater uptake and irrigation water redistribution within the potato root zone. Agric. Water Manage. 132, 101–110.
Scanlon, B.R., Christman, M., Reedy, R.C., Porro, I., Simunek, J., Flerchinger, G.N., 2002. Intercode comparisons for simulating water balance of surficial sediments in semiarid regions. Water Resour. Res. 38 (12), 1323–1339.
Schaap, M.G., Leij, F.J., van Genuchten, M.T., 2001. Rosetta: a computer program for estimating soil hydraulic parameters with hierarchical pedotransfer function. J. Hydrol. 251, 163–176.
Schreckenberg, K., Awono, A., Degrande, A., Mbosso, C., Ndoye, O., Tchoundjeu, Z., 2006. Domesticating indigenous fruit trees as a contribution to poverty reduction. For. Trees Livelihoods 16, 35–51.
Shah, N., Nachabe, M., Ross, M., 2007. Extinction depth and evapotranspiration from ground water under selected land covers. Ground Water 45 (3), 329–338.
Šimůnek, J., Šejna, M., Saito, H., Sakai, M., van Genuchten, M. T., 2013. The Hydrus-1D software package for simulating the movement of water, heat, and multiple solutes in variably saturated media, version 4.16, HYDRUS Software Series 3. Department of Environmental Sciences, University of California Riverside, Riverside, California, USA, pp. 340.
Skaggs, T.H., Shouse, P.J., Poss, J.A., 2006. Irrigation forage crops with saline waters: 2. Modeling root uptake and drainage. Vadose Zone J. 5, 824–837.
Sommer, B., Froend, R., 2014. Phreatophytic vegetation responses to groundwater depth in a drying Mediterranean-type landscape. J. Veg. Sci. 25, 1045–1055.
Soylu, M.E., Istanbulluoglu, E., Lenters, J.D., Wang, T., 2011. Quantifying the impact of groundwater depth on evapotranspiration in a semi-arid grassland region. Hydrol. Earth Syst. Sci. 15, 787–806.
Stromberg, J.C., Tiller, R., Richter, B., 1996. Effects of groundwater decline on riparian vegetation of semiarid regions: The San Pedro, Arizona. Ecol. Appl. 6, 113–131.
Sutanto, S.J., Wenninger, J., Coenders-Gerrits, A.M.J., Uhlenbrook, S., 2012. Partitioning of evaporation into transpiration, soil evaporation and interception: a comparison between isotope measurements and a HYDRUS-1D model. Hydrol. Earth Syst. Sci. 16, 2605–2616.
Sutanudjaja, E.H., van Beek, L.P.H., de Jong, S.M., van Geer, F.C., Bierkens, M.F.P., 2011. Large-scale groundwater modeling using global datasets: a test case for the Rhine-Meuse basin. Hydrol. Earth Syst. Sci. 15, 2913–2935.
Tilahun, K., 2006. Analysis of rainfall climate and evapo-transpiration in arid and semi-arid regions of Ethiopia using data over the last half a century. J. Arid Environ. 64, 474–487.
Tóth, J., 1963. A theoretical analysis of groundwater flow in small drainage basins. J. Geophys. Res. 68 (16), 4785–4812.
Tucker, C.J., Dregne, H.E., Newcomb, W.W., 1991. Expansion and contraction of the Sahara Desert from 1980 to 1990. Science 253 (5017), 299–301.
van Dam, J.C., Huygen, J., Wesseling, J.G., Feddes, R.A., Kabat, P., van Walsum, P.E. V., Groenendijk, P., van Diepen, C.A., 1997. Theory of SWAP version 2.0, Report 71. Dept. of Water Resour., Wageningen Agricultural University, Wageningen, The Netherlands.
van Genuchten, M.T., 1980. A closed-form equation for predicting the hydraulic conductivity of unsaturated soils. Soil Sci. Soc. Am. J. 44, 892–898.
van Genuchten, M.T., 1987. A Numerical Model for Water and Solute Movement in and Below the Root Zone, Research Report. US Salinity Laboratory, USDA, Riverside, California.
Wang, L., Mu, Y., Zhang, Q., Zhang, X., 2013. Groundwater use by plants in a semi-arid coal-mining area at the Mu Us Desert frontier. Environ. Earth Sci. 69, 1015–1024.
Wang, X.P., Berndtsson, R., Li, X.R., Kang, E.S., 2004. Water balance change for a re-vegetated xerophyte shrub area. Hydrol. Sci. J. 49 (2), 283–295.
Wang, P., Song, X., Han, D., Zhang, Y., Liu, X., 2010. A study of root water uptake of crops indicated by hydrogen and oxygen stable isotopes: a case in Shanxi Province, China. Agric. Water Manage. 97, 475–582.
Wang, Y., Wang, L., Wei, S., 2012. Modeling canopy rainfall interception of a replanted *Robinia pseudoacacia* forest in the Loess Plateau. Acta Ecol. Sin. 32 (17), 5445–5453 (in Chinese with English abstract).
Waring, R.H., Schlesinger, W.H., 1985. Forest Ecosystems – Concept and Management. Academic Press, Orlando.
Wenninger, J., Beza, D.T., Uhlenbrook, U., 2010. Experimental investigations of water fluxes within the soil–vegetation–atmosphere systems: stable isotope mass-balance approach to partition evaporation and transpiration. Phys. Chem. Earth 35, 565–570.
White, W.N., 1932. A method of estimating ground-water supplies based on discharge by plants and evaporation from soil: results of investigations in Escalante Valley, Utah. US Geol. Surv. Water Supply Pap. 659-A.
Xiao, Q., McPherson, E.G., Ustin, S.L., Grismer, M.E., 2000. A new approach to modeling tree rainfall interception. J. Geophys. Res. 105 (D23), 29173–29188.
Xie, T., Liu, X., Sun, T., 2011. The effects of groundwater table and flood irrigation strategies on soil water and salt dynamics and reed water use in the Yellow River Delta, China. Ecol. Model. 222, 241–252.
Yang, J., Wan, S., Deng, W., Zhang, G., 2007. Water fluxes at a fluctuating water table and groundwater contributions to wheat water use in the lower Yellow River flood plain, China. Hydrol. Process. 21, 717–724.
Yaseef, N.R., Yakir, D., Rotenberg, E., Schiller, G., Cohen, S., 2009. Ecohydrology of a semi-arid forest: partitioning among water balance components and its implications for predicted precipitation changes. Ecohydrology 3 (2), 143–154.
Yin, L.H., Zhou, Y.X., Ge, S.M., Wen, D.G., Zhang, E.Y., Dong, J.Q., 2013. Comparison and modification of methods for estimating evapotranspiration using diurnal groundwater level fluctuations in arid and semiarid regions. J. Hydrol. 496, 9–16.
Yin, L.H., Zhou, Y.X., Huang, J.T., Wenninger, J., Hou, G.C., Zhang, E.Y., Wang, X.Y., Dong, J.Q., Zhang, J., Uhlenbrook, S., 2014. Dynamics of willow tree (*Salix*

matsudana) water use and its response to environmental factors in the semi-arid Hailiutu River Catchment, Northwest China. Environ. Earth Sci. 71 (12), 4997–5006.

Zencich, S.J., Froend, R.H., Turner, J.V., Gailitis, V., 2002. Influence of groundwater depth on the seasonal sources of water accessed by *Banksia* tree species on a shallow, sandy coastal aquifer. Oecologia 131, 8–19.

Zhang, Y., Shen, Y., Sun, H., Gates, J.B., 2011. Evapotranspiration and its partitioning in an irrigated winter wheat field: A combined isotopic and micrometeorologic approach. J. Hydrol. 408, 203–211.

Zhao, W.Z., Liu, B., 2010. The response of sap flow in shrubs to rainfall pulses in the desert region of China. Agric. For. Meteorol. 150, 1297–1306.

Zhou, Y., Wenninger, J., Zhi, Y., Yin, L., Huang, J., Hou, L., Wang, X., Zhang, D., Uhlenbrook, S., 2013. Groundwater–surface water interactions, vegetation dependencies and implications for water resources management in the semi-arid Hailiutu River catchment, China – a synthesis. Hydrol. Earth Syst. Sci. 17, 2435–2447.

Zhu, Y., Ren, L., Skaggs, T.H., Lü, H., Yu, Z., Wu, Y., Fang, X., 2009. Simulation of *Populus euphratica* root uptake of groundwater in an arid woodland of the Ejina Basin, China. Hydrol. Process. 23, 2460–2469.

Zimmermann, U., Ehhalt, D., Munnich, K.O., 1967. Soil-water movement and evapotranspiration: changes in the isotopic composition of the water. Proceedings of the Symposium of Isotopes in Hydrology, Vienna, Austria, IAEA.

Zinke, P.J., 1967. Forest interception study in the United Stages. In: Sopper, W.E., Lull, H.W. (Eds.), Forest Hydrology. Pergamon, Tarrytown, pp. 137–161.

Zribi, M., Le Hégarat-Mascle, S., Tacone, O., Ciarletti, V., Vidal-Madjar, D., Boussema, M.R., 2003. Derivation of wild vegetation cover density in semi-arid regions. Int. J. Remote Sens. 24, 1335–1352.